THE ASTROPHYSICAL JOURNAL, 491:515–521, 1997 December 20

X-RAY SPECTRUM OF THE HIGH-POLARIZATION QUASAR PKS 1510−089

K. P. SINGH,[1,2] C. R. SHRADER,[3,4,5] AND I. M. GEORGE[3,4,6]

Received 1997 May 30; accepted 1997 July 30

ABSTRACT

We present results from the X-ray spectra of the radio-loud, high-polarization quasar PKS 1510−089, based on new data obtained using *ASCA* and from archival *ROSAT* data. We find the X-ray spectrum obtained by *ASCA* to be unusually hard, with the photon index $\Gamma = 1.30 \pm 0.06$, while the (nonsimultaneous) *ROSAT* data indicate a steeper spectrum with $\Gamma = 1.9 \pm 0.3$. However, we find the X-ray flux at 1 keV to be within $\sim 10\%$ during both observations. Thus, we suggest the most likely explanation is that there is a break (with $\Delta\Gamma \geq 0.6$) in the underlying continuum at ~ 0.7 keV.

Although the sample of high-polarization quasars for which high-quality X-ray spectra are available is small, flat X-ray spectra seem to be characteristic of these objects, and they also appear to be harder than that of the other radio-loud but low-polarization quasars. The multiwavelength spectrum of PKS 1510−089 is similar to many other γ-ray blazars, suggesting the emission is dominated by that from a relativistic jet. A big blue bump is also seen in its multiwavelength spectrum, suggesting the presence of a strong thermal component as well.

Subject headings: galaxies: active — galaxies: nuclei — polarization — quasars: individual (PKS 1510−089) — radiation mechanism: nonthermal — X-rays: galaxies

1. INTRODUCTION

High-polarization quasars (HPQs), along with BL Lac objects, form a subset of active galactic nuclei (AGNs) known as blazars. HPQs are among the most energetic AGNs. They are characterized by strong and variable radio, infrared, and optical continuum emission with a high degree of polarization. Blazars are also strong and variable soft X-ray emitters (Brunner et al. 1994), and they recently have also been found to emit ≥ 100 MeV γ-rays (Thompson et al. 1993). The X-ray spectral measurements of blazars have shown that the HPQs tend to have flatter spectral indices than the BL Lac objects (Sambruna et al. 1994). The uncertainties in these measurements of spectral indices are, however, generally large due to the small bandwidth, poor sensitivity, and low-energy absorption in the interstellar medium. There is also a general dearth of broadband spectral measurements of HPQs extending to hard X-rays, the few exceptions being 3C 279 and 3C 345 (Makino 1989), PKS 1510−089 (Singh, Rao, & Vahia 1990), PKS 0537−441 (Sambruna et al. 1994), 3C 390.3 (Eraclous, Halpern, & Livio 1996), and a serendipitous detection of PKS 1502+106 (George et al. 1994). We chose to carry out X-ray spectral measurements of PKS 1510−089 with *ASCA*, as previous measurements with *EXOSAT*, reported by Singh et al. (1990) and Sambruna et al. (1994), indicated an unusually flat X-ray spectrum.

Radio source PKS 1510−089 was first identified optically as a quasar with an ultraviolet excess, a visual magnitude of 16.5 (Bolton & Ekers 1966), and a redshift of $z = 0.361$ measured from its emission-line spectrum (Burbidge & Kinman 1966). Optical polarimetric observations by Appenzeller & Hiltner (1967) detected strong ($10.9\% \pm 3.8\%$) polarization at a position angle of $177° \pm 9°$. The strong variability of its optical brightness was first reported by Lu (1972), who monitored it for 5 yr. Subsequently, it was found that its *B* magnitude had varied by ~ 6 mag since 1899.6 (Liller & Liller 1975). *The range of brightness spanned is larger than that known for any other quasar*. Its radio emission exhibits very rapid, large amplitude variations in both total and polarized flux (Aller, Aller, & Hodge 1981; Aller, Aller, & Hughes 1996). It is a core-dominated radio source with a *one-sided* jet that subtends about 8″.0 in the 20 cm wave band (O'Dea, Barvainis, & Challis 1988). Strong infrared (see Landau et al. 1986), millimeter (see Steppe et al. 1988), and UV emission (Malkan & Moore 1986) have also been detected from PKS 1510−089. γ-ray emission from PKS 1510−089 has also been detected by the *EGRET* instrument on *Compton Gamma Ray Observatory* (Thompson et al. 1993; Sreekumar et al. 1996) with a flux of $2.3 \pm 0.57 \times 10^{-7}$ photons cm^{-2} s^{-1} for γ-rays with energies ≥ 100 MeV and a photon spectral index of 2.51 ± 0.36.

The broadband X-ray observations in 1984 and 1985 with *EXOSAT*, described by Singh et al. (1990), showed that its X-ray spectrum is best fitted by a power law with a photon index $\Gamma = 1.40 \pm 0.35$ and low-energy absorption consistent with the Galactic value of N_H in its direction (8.1×10^{20} cm^{-2}) as given by Stark et al. (1992). The 2–10 keV flux from *EXOSAT* observations was found to be 8.9×10^{-12} ergs cm^{-2} s^{-1} in the observer's frame. The source is highly luminous, with its X-ray luminosity alone being $\simeq 7 \times 10^{45}$ ergs s^{-1}, assuming isotropic emission, redshift of 0.361, $H_0 = 50$ km s^{-1} Mpc^{-1}, and $q_0 = 0$ in the Friedmann cosmology.

In this letter, we present new *ASCA* observations of PKS 1510−089, along with an analysis of archival *ROSAT* data.

[1] X-Ray Astronomy Group, Tata Institute of Fundamental Research, Mumbai 400 005, India.
[2] singh@tifrvax.tifr.res.in.
[3] Laboratory for High Energy Astrophysics, NASA/GSFC, Greenbelt, MD 20771.
[4] Also Universities Space Research Association, 7501 Forbes Boulevard, Seabrook, MD 20706.
[5] shrader@grossc.gsfc.nasa.gov.
[6] ian.george@gsfc.nasa.gov.

Details of the observations and data reduction are given in § 2 and the results from the spectral analysis in § 3. We discuss our findings in § 4.

2. OBSERVATIONS AND DATA REDUCTION

2.1. *ASCA*

PKS 1510−089 was observed with *ASCA* on 1996 August 20 as part of the Guest Observer Program (see Table 1 for the log of observations). The *ASCA* observatory (Tanaka et al. 1994) contains four imaging thin–foil grazing incidence X-ray telescopes, two of which are equipped with Solid State Imaging Spectrometers (SIS) and the other two with Gas Imaging Spectrometers (GIS). SIS detectors have been described in detail by Burke et al. (1991), and GIS by Ohashi et al. (1996) and Makishima et al. (1996). Their properties have been summarized, e.g., in Singh, White, & Drake (1996). Because of radiation damage since the launch of *ASCA*, at the time of the observations reported here the spectral resolution of the SIS detectors had been degraded to ∼10% at 1 keV. This spectral resolution is taken into account by the response matrix generated as part of the analysis of this spectrum.

The data were selected as described in Singh et al. (1996) using the FTOOLS/XSELECT software package. PKS 1510−089 is the only source detected in the field of view. The counts and pulse height spectra were accumulated from a source region of 4′ radius in the SIS and 6′ radius in the GIS, while the background was taken from the off-axis source-free regions in the SIS and GIS where counts from the outer wings of the point-spread function of the source were minimized. The source spectra were grouped to have a minimum of 20 counts per energy channel prior to spectral analysis (see § 3). We have compared our results with those obtained assuming background spectra accumulated from deep observations of blank sky and obtain consistent results (within statistical uncertainties).

Steady X-ray emission from PKS 1510−089 was detected with a count rates of ∼0.18 and ∼0.14 counts s^{-1} above background in SIS0 and SIS1 detectors and in energy bands of 0.5–8.2 keV and 0.65–8.0 keV, respectively. Similarly, the count rates observed with GIS2 and GIS3 were ∼0.12 and ∼0.14 counts s^{-1} in the energy bands of 0.75–9.7 keV and 0.70–10.0 keV, respectively. No significant variability was seen on timescales of minutes to hours in any of the detectors. The average X-ray flux in the 0.4–10 keV energy band in the observer's frame was $\sim 1.1 \times 10^{-11}$ ergs cm^{-2} s^{-1}, which implies an X-ray luminosity of $\sim 10^{46}$ ergs s^{-1} ($z = 0.361$, $H_0 = 50$ km s^{-1} Mpc^{-1}, $q_0 = 0$ in the Friedmann cosmology). Similarly, the 2–10 keV flux in the observer's frame was 8.6×10^{-12} ergs cm^{-2} s^{-1}, which is within 4% of the value observed with *EXOSAT*, consistent with the uncertainties in the cross-calibration of the absolute fluxes of the two satellites. The flux estimates are based on the best-fit spectral models described in § 3.

2.2. *ROSAT*

PKS 1510−089 was detected in the *ROSAT* all-sky survey (RASS), as well as during the pointed observations (Siebert et al. 1995). We have retrieved the publicly available *ROSAT* data from the pointed observations from the archives maintained at NASA High-Energy Astrophysics Science Archive Research Center (HEASARC). The pointed observations were carried out on 1992 August 17 as part of the *ROSAT* Guest Observer Program, utilizing a position sensitive proportional counter (PSPC) as the focal plane detector (Trümper 1983; Pfeffermann et al. 1987). The PSPC has a field of view of 2°, an energy resolution (FWHM) of 0.42% at 1 keV, and a nominal (gain sensitive) bandwidth for greater than 10% efficiency of 0.1–2.0 keV. No other X-ray source was detected in the neighborhood of PKS 1510−089. The details of the observations are given in Table 1. The on-source counts were selected from a circular region having a radius of about 3′.25 and centered on the source. An X-ray spectrum from the region was accumulated for the entire observation. The background was accumulated from several neighboring regions at approximately the same offset as the source. The spectral data from the source were binned from the original 256 channels by grouping the first 176 channels by 8 and the rest by 16 to improve the signal–to–noise ratio (S/N) in each energy bin. These observations resulted in a reasonably good quality spectra with typical S/N per bin of 5 σ.

Steady soft X-ray emission from PKS 1510−089 was detected with a count rate of ∼0.18 counts s^{-1} above background in the energy range of 0.13–2.0 keV in the observer's frame. According to Siebert et al. (1995), the source flux changed by a factor of ∼3.5 between the RASS and the pointed mode observation about 2 yr later. The average X-ray flux in the 1992 pointed mode observation in the 0.1–2 keV energy band was 2.1×10^{-12} ergs cm^{-2} s^{-1} in the observer's frame. The flux estimate is based on the best-fit spectral models in § 3.

3. SPECTRAL ANALYSIS AND RESULTS

3.1. *ASCA*

We have analyzed the X-ray spectra obtained from SIS data for $E \geq 0.5$ keV and the GIS data for energies ≥0.7 keV. The spectra were analyzed using XSPEC v9.0 (Arnaud 1996). We first analyzed the data from each detector separa-

TABLE 1

OBSERVATION LOG FOR PKS 1510−089

Satellite Name	Detector Name	Date	Exposure (s)	Count Rate[a] (counts s^{-1})	Energy Range[b] (keV)
ROSAT.....	PSPC	1992 Aug 17	5153	0.176 ± 0.006	0.13–1.9
ASCA.....	SIS0	1996 Aug 20	18317	0.180 ± 0.004	0.51–8.2
ASCA.....	SIS1	1996 Aug 20	18105	0.141 ± 0.003	0.65–8.0
ASCA.....	GIS2	1996 Aug 20	18301	0.118 ± 0.003	0.75–9.7
ASCA.....	GIS3	1996 Aug 20	18300	0.138 ± 0.003	0.70–10.0

[a] After background subtraction.
[b] In observer frame.

TABLE 2

RESULTS FROM ANALYSIS OF SIS AND GIS SPECTRA

Model	N_H (10^{20} cm^{-2})	Γ_h	A[a]	Γ_l or kT_{bb}[b] or pcf[c]	E_{bk} or L_{bb}[d]	χ^2/dof	E_l (keV)	EW (eV)
Power law	$16.0^{+4.0}_{-3.7}$	$1.30^{+0.06}_{-0.06}$	11.2	...	...	458.3/444	...	...
Power law + Gaussian	$16.6^{+3.4}_{-3.6}$	$1.32^{+0.03}_{-0.05}$	11.4	...	...	453.5/442	5.1 ± 0.5	87
Broken power law	$17.2^{+6.1}_{-4.8}$	$1.31^{+0.07}_{-0.06}$	10.8	$1.8^{+1.1}_{-1.4}$	0.9	458.1/442	...	...
Broken power law + Gaussian	$18.0^{+5.0}_{-3.0}$	$1.33^{+0.06}_{-0.05}$	11.7	$1.8^{+1.3}_{-1.3}$	0.9	453.1/440	5.1 ± 0.5	88
Power law + blackbody	$11.3^{+5.0}_{-3.5}$	$1.07^{+0.17}_{-0.10}$	7.6	0.45	<1.0	452.2/442	...	...
Partially covered power law[e]	32^{+80}_{-25}	$1.31^{+0.08}_{-0.07}$	11.3	$0.54^{+0.46}_{-0.31}$	...	458.4/443	...	...

NOTE.—Errors and upper limits are with 90% confidence based on $\chi^2_{min} + 2.71$.

[a] Unabsorbed flux at 1 keV (observer frame) in units of 10^{-4} photons cm^{-2} s^{-1} keV^{-1}.

[b] Γ_2: Low-energy photon index. kT_{bb}: Blackbody temperature in keV.

[c] pcf: Partially covering fraction of the source.

[d] E_{bk}: Break energy in keV for the broken power law. L_{bb}: Total blackbody luminosity in 10^{44} ergs s^{-1}.

[e] Fixed $N_H = 8.1 \times 10^{20}$ cm^{-2} due to galaxy + absorption at $z = 0.361$.

tely using a simple absorbed power-law model with absorption cross sections and abundances from Morrison & McCammon (1983) and Anders & Grevesse (1989). The spectra SIS0, SIS1, GIS2, and GIS3 all gave consistent results. The analysis was then performed jointly on the two SIS detectors, on the two GIS detectors; and finally on all four detectors jointly. We fit the spectra from all four instruments simultaneously, but we allow the normalization of the model to be free for each detector to account for differences in the absolute flux calibrations of the instruments. The results based on the joint analyses of all four detectors are given in Table 2. The results are consistent with the analysis of spectra from individual detectors, analyzed separately. The observed spectra from the four detectors along with the best-fit model of an absorbed power law are shown separately for SIS detectors in Figure 1 and for GIS detectors in Figure 2. The fit is very good, having a reduced χ^2 statistic of $\chi^2_\nu = 1.03$. The resulting spectrum is hard with a photon index of $\Gamma = 1.30^{+0.06}_{-0.06}$ (where the errors are at 90% confidence for one parameter of interest) and an equivalent hydrogen column density estimated from low-energy absorption of $N_H = 16 \pm 4 \times 10^{20}$ cm^{-2}, which is about twice that due to absorption in our galaxy (see § 1). The same result is obtained if assume an absorber at $z = 0.361$, along with a fixed absorption from 21 cm measurements in our Galaxy. In Figure 3 we show the 68%, 90%, and 99% confidence contours for the values of the spectral index and the N_H allowed by the data. Motivated by an earlier report about the presence of a Gaussian feature near 5 keV in the spectrum (Singh et al. 1990), we also tried adding a similar feature to the *ASCA* spectra and got a marginal improvement in the quality of the fit. The best-fit line position was at

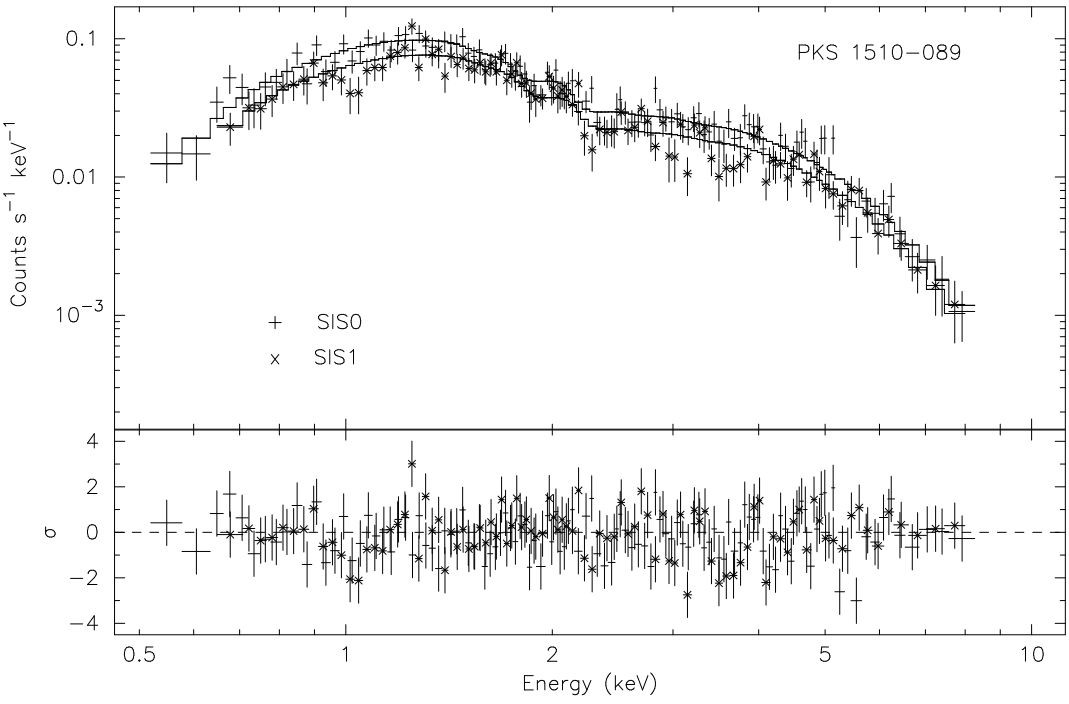

FIG. 1.—Best-fit SIS spectra from a joint fit to the SIS and GIS spectra are shown after fitting with a single absorbed power law (*upper panel*). The best-fit model is shown as a histogram. The departures from the best fit are shown in the lower panel as the number of σ's with an error bar of 1 σ.

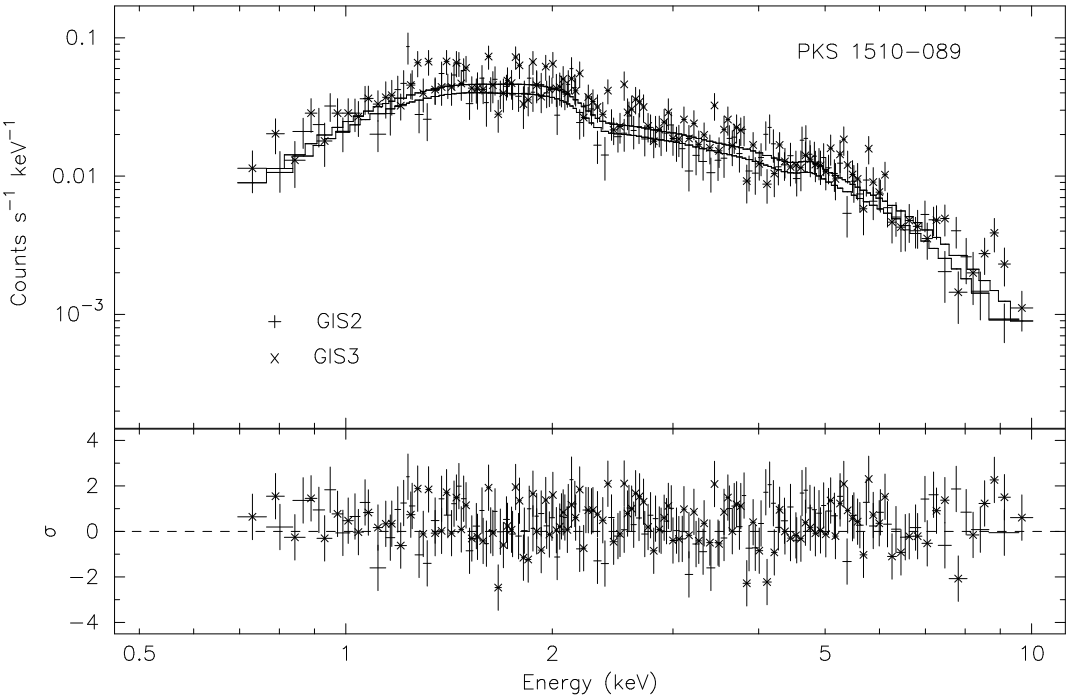

FIG. 2.—Same as in Fig. 1, but for the GIS spectra

5.1 ± 0.5 keV, with an equivalent width of about 87 eV. Considering the S/N in this portion of the spectrum and the fact that the overall fit improved only marginally, we regard this equivalent width as an upper limit. The equivalent width of the emission line suggested by an *EXOSAT* observation (Singh et al. 1990) was several times higher, suggesting either that the line varied or that it was spurious. Alternate models, e.g., (1) a broken power law with a low-energy index Γ_l, a break at energy $E_c \sim 0.9$ keV, and a high-energy index Γ_h; or (2) the addition of a blackbody to a simple power law; or (3) a partially covered power law, provided equally good fits to the spectra (see Table 2). The improvement in the fit was insignificant, however. Therefore, the data are not able to distinguish between the absence or the presence of a low-energy excess in the spectrum.

3.2. *ROSAT*

Results from our spectral analysis of the *ROSAT* PSPC data are presented in Table 3. A simple absorbed power-law model provided a good fit to the PSPC spectrum. The data and our best-fit power-law model are shown in Figure 4. The confidence contours for the spectral index and the hydrogen column density, $N_{\rm H}$, allowed by the PSPC data are shown in Figure 3. The best-fit spectral index, $\Gamma = 1.88 \pm 0.28$, is significantly higher than that measured

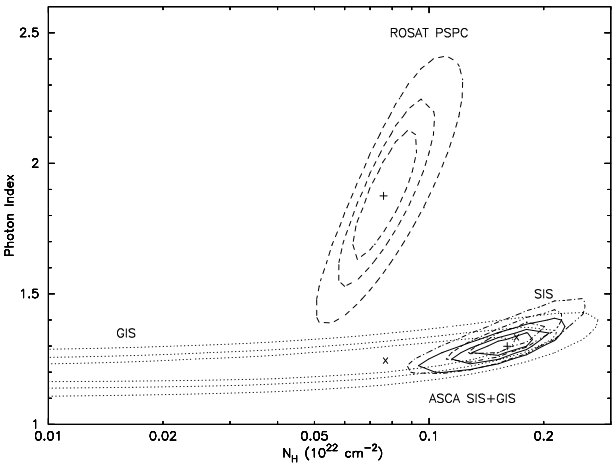

FIG. 3.—Allowed ranges of the $N_{\rm H}$ and Γ from the X-ray spectrum of PKS 1510−089 based on the χ^2 contours. The full contours represent the 68%, 90%, and 99% confidence limits from fitting SIS + GIS together, the dash-dotted contours show similar confidence levels for the SIS data alone, the dotted contours are for the GIS data alone, and the dashed contours are for the PSPC data alone. The plus signs and crosses mark the best-fit values.

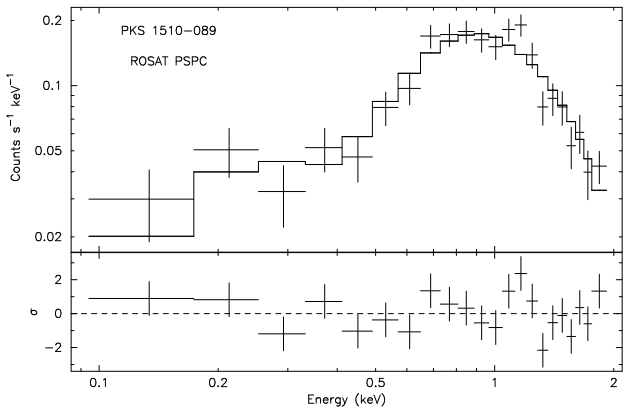

FIG. 4.—Best-fit PSPC spectra using a single absorbed power law, shown in the same way as for Figs. 1 and 2.

TABLE 3

RESULTS FROM ANALYSIS OF PSPC SPECTRUM

Spectrum No.	Model	N_H (10^{20} cm^{-2})	Γ_h	A[a]	Γ_l or kT_{bb}[b]	E_{bk} or L_{bb}[c]	χ^2/dof	F_{SX}[d]	L_{SX}[e]
1.....	Power law	$7.6^{+2.0}_{-1.5}$	1.88 ± 0.28	10.2	...	...	25.9/20	2.1	3.5
2.....	Broken power law	$7.7^{+2.0}_{-1.7}$	1.30	10.2	1.9 ± 0.2	$1.6^{+\inf}_{-0.4}$	25.6/19	2.1	3.6
3.....	Power law + blackbody	$5.1^{+1.5}_{-1.3}$	1.30	6.2	0.21 ± 0.05	7.0 ± 4.0	24/18	2.0	2.2

NOTE.—Errors and upper limits are with 90% confidence based on $\chi^2_{min} + 2.71$.
[a] Unabsorbed flux at 1 keV (observer frame) in units of 10^{-4} photons cm^{-2} s^{-1} keV^{-1}.
[b] Γ_2: Low-energy photon index. kT_{bb}: Blackbody temperature in keV.
[c] E_{bk}: Break energy in keV for the broken power-law. L_{bb}: Total blackbody luminosity in 10^{44} ergs s^{-1}.
[d] Absorbed flux between 0.1–2.0 keV (observer frame) in units of 10^{-12} ergs cm^{-2} s^{-1}.
[e] Intrinsic luminosity (no absorption) between 0.1–2.0 keV (observer frame) in units of 10^{45} ergs s^{-1}.

during the *ASCA* observations. The corresponding column density, N_H, is $7.6^{+2.0}_{-1.5} \times 10^{20}$ cm^{-2}, which is consistent with the 21 cm value. The unabsorbed flux at 1 keV is $\sim$10% lower than in the *ASCA* observations. The apparent discrepancy between the *ROSAT* and *ASCA* observations imply either that variations in both the spectral index and the absorbing column occurred between the two epochs or that the PSPC band is dominated by a separate, steep spectral component. The PSPC spectra could be fit equally well by a broken power law ($\Gamma_l = 1.9 \pm 0.2$, with the hard component fixed at $\Gamma_h = 1.30$) with absorption; however, the break energy cannot be constrained (see Table 3). A model consisting of a low-energy blackbody and hard power law also provides a statistically acceptable description of the data. However, such a model requires a value of N_H less than the Galactic value, and hence we consider it unrealistic. The PSPC data show no preference for any of the three models.

3.3. *ROSAT and ASCA Combined Spectral Analysis*

If we accept the simple absorbed power law, then there is a significant difference between the spectral index and N_H observed by *ROSAT* in 1992 compared with that observed by *ASCA* 4 yr later. Since there were no measurements above 2 keV in 1992, the hard X-ray flux seen with *ASCA* might have varied even though the 1 keV flux hardly changed. In that case, joint fitting of *ROSAT* and *ASCA* data would not be meaningful. In the likely case that a more complex spectrum is present with a change around 1 keV, the joint fitting can constrain the additional parameters involved in multicomponent models. We, therefore, carried out multicomponent, multi-instrument model fitting, the results of which are given in Table 4. We fit the spectra from all five instruments simultaneously, but we allow the normalization of the model to be free for each detector to account for differences in the absolute flux calibrations of the instruments and changes in source intensity between the two epochs. As expected, a simple power-law model gives an acceptable fit only if the N_H is allowed to be significantly lower than the Galactic value in the direction of PKS 1510−089. Both the broken power-law and blackbody plus power-law models give acceptable fits to the data, with the N_H value almost consistent with the Galactic value (see Table 4). A partially covered power-law model with Galactic absorption and a very high absorption intrinsic to the source at $z = 0.361$ gives a somewhat poorer fit. Thus, we conclude that the most likely explanation of the *ROSAT* and *ASCA* observations is that a power law of photon index $\Gamma \simeq 1.3$ dominates the spectrum above $\gtrsim 1$ keV with a 2–10 keV flux $\simeq 8.6 \times 10^{-12}$ ergs cm^{-2} s^{-1} at both epochs in the observer's frame. A separate, steeper spectral component dominates at lower energies, the specific form of which cannot be unambiguously determined.

4. DISCUSSION

ASCA observations show that the 0.5–10 keV X-ray spectrum of PKS 1510−089 is hard ($\Gamma \simeq 1.3$). Although earlier observations with *EXOSAT* (Singh et al. 1990; Sambruna et al. 1994) had indicated that the X-ray spectrum of PKS 1510−089 might be this hard, those measurements were not conclusive because of a relatively poor S/N. The observed spectral index is significantly flatter than that

TABLE 4

RESULTS FROM JOINT ANALYSIS OF PSPC, SIS, AND GIS SPECTRA

Model	N_H (10^{20} cm^{-2})	Γ_h	A[a]	Γ_l or kT_{bb}[b] or pcf[c]	E_{bk} or L_{bb}[d]	χ^2/dof
Power law	$5.1^{+1.1}_{-0.7}$	$1.17^{+0.04}_{-0.03}$	9.3	...	...	531.2/466
Broken power law	$11.3^{+3.0}_{-3.0}$	$1.24^{+0.04}_{-0.04}$	4.9	$3.5^{+0.0}_{-1.2}$	$0.70^{+0.10}_{-0.10}$	520.7/464
Power law + blackbody	$11.8^{+2.0}_{-1.6}$	$1.25^{+0.05}_{-0.05}$	10.4	$0.056^{+0.01}_{-0.01}$	7.6	520.3/464
Partially covered power law[e]	200^{+220}_{-50}	$1.30^{+0.17}_{-0.05}$	11.3	$0.15^{+0.75}_{-0.12}$	...	538.1/465

NOTE.—Errors and upper limits are with 90% confidence based on $\chi^2_{min} + 2.71$.
[a] Unabsorbed flux at 1 keV (observer frame) in units of 10^{-4} photons cm^{-2} s^{-1} keV^{-1}.
[b] Γ_2: Low-energy photon index. kT_{bb}: Blackbody temperature in keV.
[c] pcf: Partially covering fraction of the source.
[d] E_{bk}: Break energy in keV for the broken power law. L_{bb}: Total blackbody luminosity in 10^{45} ergs s^{-1}.
[e] Fixed $N_H = 8.1 \times 10^{20}$ cm^{-2} due to galaxy + absorption at $z = 0.361$.

of the typical radio-loud quasars ($\langle\Gamma\rangle = 1.66 \pm 0.07$: Lawson et al. 1992; Cappi et al. 1997), radio-quiet quasars ($\langle\Gamma\rangle = 1.90 \pm 0.11$: Lawson et al. 1992; Williams et al. 1992), and BL Lac objects ($\langle\Gamma\rangle = 2.20^{+0.17}_{-0.15}$: Sambruna et al. 1994). The observed spectrum is, however, similar to that of other HPQs observed in both the hard (e.g., 3C 345 with $\Gamma = 1.4 \pm 0.09$: Makino 1989; PKS 0537−441 with $\Gamma = 1.26^{+0.24}_{-0.31}$: Sambruna et al. 1994) and the soft (e.g., 0212+735 with $\Gamma = 0.44^{+0.39}_{-0.41}$ and 0836+710 with $\Gamma = 1.4 \pm 0.05$: Brunner et al. 1994) X-ray bands. Thus, based on an admittedly small number of examples, HPQs do appear to show X-ray spectra that are flatter than those of other core-dominated radio-loud quasars.

PKS 1510−089 was observed in the near-ultraviolet band with the *International Ultraviolet Explorer* (*IUE*) low-dispersion spectrographs during the early 1980s. There are three SWP exposures and two LWR exposures in the archive. The SWPs include one nondetection and two spectra obtained over a nominal 1 yr baseline whose continuum levels are equivalent to the 1 σ level. One LWR exposure was underexposed and resulted in a nondetection. There is, however, no evidence of variability in the available UV data, although it cannot be ruled out either. Though weakly detected on one occasion with the short- and long-wavelength instruments, redshifted emission lines of Lyα and O VI/Lyβ are clearly detected, with several other normally prominent emission lines possibly present. The UV continuum is well approximated by a power law with index -1.2 (ν vs. f_ν).

We constructed a multifrequency spectrum using measurements from the published literature. The spectrum is shown in Figure 5. We note that these data do not result from simultaneous or even contemporaneous observations. The "radio" points at 1.5 and 4.9 GHz are from O'Dea et al. (1988); we note however that Aller et al. (1996), who present a 20 yr radio light curve for PKS 1510−089, show that it varies by at least a factor of 5, mainly in series of flarelike events occurring on yearly timescales (and sometimes persisting for months). The near-IR measurement at 1.5 μm is from Landau et al. (1986), and we used the visual magnitude of $V = 16.5$ of Bolton & Elkers (1966) to derive a flux point corresponding to 5500 Å. We used the UV measurements obtained from the *IUE* archives as described previously. The optical and UV fluxes have been corrected for galactic extinction using the extinction law of Seaton (1979) and a color excess estimated from the galactic N_H values derived from the 21 cm measurements. The γ-ray flux at energies ≥ 100 MeV has been taken from *EGRET* measurements (Thompson et al. 1993).

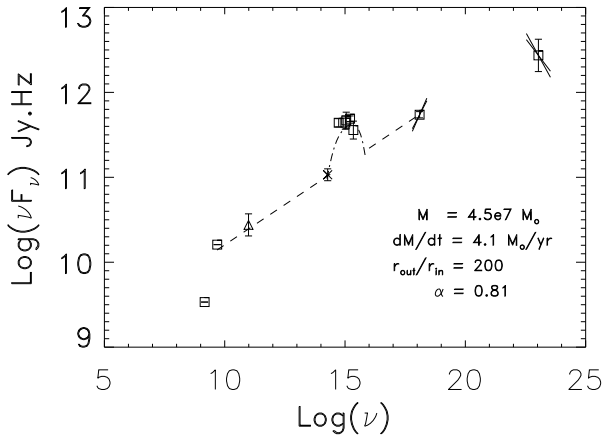

FIG. 5.—Broadband spectral energy distribution of PKS 1510−089 based on the (noncontemporaneous) multifrequency measurements cited in the text. The dotted line represents a power-law fit to the millimeter, IR, and X-ray measurements, with a superposed multicolor blackbody disk fit to the apparent blue-bump residual. The outer disk radius required to obtain the fit was much smaller than is normally the case for radio-quiet AGN—we suspect that the actual optical flux at the time of the UV measurements was probably higher.

The multi–wave-band spectrum of PKS 1510−089 resembles that of many other blazars detected by *EGRET*, with the bulk of the luminosity being emitted as γ-rays (e.g., see Fig. 5 of von Montigny et al. 1995—indeed, we note the multi–wave-band spectrum of PKS 1510−089 is globally very similar to the BL Lac Mrk 421). In the popular relativistic jet models, the hard X-ray and γ-ray emission is proposed to arise as a result of inverse Compton scattering of low-energy photons by relativistic electrons within the jet (e.g., see von Montigny et al. 1995 and references therein). We suggest that the double power-law form found above might indicate that the *ROSAT* data are dominated by the steep tail of this low-energy emission (often assumed to be synchrotron radiation), while the flatter inverse-Compton-scattered component dominates the *ASCA* data greater than 1 keV. We suggest that even though superluminal motion has not (yet) been detected in this source, the emission is likely to be relativistically beamed.

Based on Figure 5, PKS 1510−089 may be among a subclass of blazar AGNs that exhibit the so-called big blue-bump component. In order to study the blue-bump emission, we subtracted a power-law component, connecting the X-ray, IR, and millimeter radio points, from the multifrequency spectrum to obtain residuals in the optical-UV region. A statistically significant, positive residual is obtained. We emphasize that variability could account for some or all of this apparent residual. We then fit a thermal accretion disk spectrum to these residual spectra. The model involves thermal emission due to viscous dissipation in a steady state, accretion disk that has been modified to include the effects of gravitational redshift and focusing (e.g., Sun & Malkan 1989); we have employed computational methods similar to those described in Czerny, Czerny, & Grindlay (1986). A Schwarzschild metric was used in the calculations, and an inclination of $\sin i = 0.5$ was assumed. We fixed the inner disk radius at $3R_g$ and $R_{\rm out}/R_{\rm in} \simeq 200$. We were unable to obtain a reasonable fit to the optical and UV data without reducing $R_{\rm out}/R_{\rm in}$ to this level; values more typically fitted to AGNs are of order $R_{\rm out}/R_{\rm in} \simeq 10^3$. Again, this could possibly be attributed to variability—we suspect that the actual visual flux at the time of the UV measurements may have been significantly higher.

If the blue-bump residual we depict here is not an artifact of nonsimultaneous measurements of a highly variable source, PKS 1510−089 is among a minority of the extreme blazar AGNs that both emit γ-rays and exhibit a blue-bump component. Another blazar with a blue-bump component is 3C 345 (e.g., Webb et al. 1994), but it was never detected at more than a 3.5 σ level with *EGRET*.

A detailed discussion of the various physical models proposed for such objects is beyond the scope of the current paper. Further simultaneous, broadband UV, X-ray, and γ-ray observations are required to constrain physical models.

We wish to thank the entire *ASCA* team for making these observations possible. This research has made use of *ROSAT* archival data obtained through the High Energy Astrophysics Science Archive Research Center (HEASARC) Online Service, provided by the NASA-Goddard Space Flight Center.

REFERENCES

Aller, H. D., Aller, M. F., & Hodge, P. E. 1981, AJ, 86, 325
Aller, M. F., Aller, H. D., & Hughes, P. A. 1996, in ASP Conf. Ser. 110, Proceedings of Blazar Continuum Variability, ed. H. R. Miller, J. R. Webb, & J. C. Noble (San Francisco: ASP), 193
Anders, E., & Grevesse, N. 1989, Geochim. Cosmochim. Acta, 53, 197
Appenzeller, I., & Hiltner, W. A. 1967, ApJ, 149, L17
Arnaud, K. A. 1996, in ASP Conf. Ser. 101, Astronomical Data Analysis Software and Systems V, ed. G. Jacoby & J. Barnes (San Francisco: ASP), 17
Bolton, J. G. & Ekers, J. 1966, Australian J. Phys., 19, 559
Brunner, H., Lamer, G., Worrall, D. M., & Staubert, R. 1994, A&A, 287, 436
Burbidge, E. M., & Kinman, T. D. 1966, ApJ, 145, 654
Burke, B. E., et al. 1991, IEEE Trans., ED-38, 1069
Cappi, M., Matsuoka, M., Comastri, A., Brinkmann, W., Elvis, M., Palumbo, G. C. C., & Vignali, C. 1997, ApJ, 478, 492
Czerny, B., Czerny, M., & Grindlay, J. E. 1986, ApJ, 311, 241
Eraclous, M., Halpern, J. P., & Livio, M. 1996, ApJ, 459, 89
George, I. M., Nandra, K., Turner, T. J., & Celotti, A. 1994, ApJ, 436, L59
Landau, R., et al. 1986, ApJ, 308, 78
Lawson, A. J., Turner, M. J. L., Williams, O. R., Stewart, G. C., & Saxton, R. D. 1992, 259, 743
Liller, M. H., & Liller, W. 1975, ApJ, 199, L133
Lu, P. K. 1972, AJ, 77, 829
Makino, F. 1989, in Proc. 23rd ESLAB Symp. on Two Topics in X-Ray Astronomy, ed. J. Hunt & B. Battrick, vol. 2 (ESA SP-296; Paris: ESA), 803
Makishima, K., et al. 1996, PASJ, 48, 171
Malkan, M. A., & Moore, R. L. 1986, ApJ, 300, 216
Morrison, R., & McCammon, D. 1983, ApJ, 270, 119
O'Dea, C. P., Barvainis, R., & Challis, P. M. 1988, AJ, 96, 435
Ohashi, T., et al. 1996, PASJ, 48, 157
Pfeffermann, E., et al. 1987, Proc. SPIE Int. Soc. Opt. Eng., 733, 519
Sambruna, R. M., Barr, P., Giommi, P., Maraschi, L., Tagliaferri, & Treves, A. 1994, ApJ, 434, 468
Seaton, M. J. 1979, MNRAS, 187, 73
Siebert, J., Brinkmann, W., Marganti, R., Tadhunter, C. N., Danziger, I. J., Fosbury, R. A. E., & di Serego Aligheri, S. 1995, MNRAS, 279, 1331
Singh, K. P., Rao, A. R., & Vahia, M. N. 1990, ApJ, 365, 455
Singh, K. P., White, N. E., & Drake, S. A. 1996, ApJ, 456, 766
Sreekumar, P., et al. 1996, ApJ, 464, 628
Stark, A. A., Gammie, C. F., Wilson, R. W., Bally, J., Linke, R. A., Heiles, C., & Hurwitz, M. 1992, ApJS, 79, 77
Steppe, H., et al. 1988, A & AS, 75, 317
Sun, W.-H., & Malkan, M. A. 1989, ApJ, 346, 68
Tanaka, Y., et al. 1994, PASJ, 46, L37
Thompson, D. J., et al. 1993, ApJ, 415, L13
Trümper, J. 1983, Adv. Space Res., 2, 241
von Montigny, C., et al. 1995, ApJ, 440, 525
Webb, J. R., et al. 1994, ApJ, 422, 570
Williams, O. R., et al. 1992, ApJ, 389, 157